Advances in Computational Mathematics
https://doi.org/10.1007/s10444-019-09680-2

Coupling the algebraic model of bypass transition with EARSM model of turbulence

Jiří Holman[1] · **Jiří Fürst**[1]

Received: 26 September 2018 / Accepted: 8 March 2019 / Published online: 26 April 2019

Abstract
The article deals with numerical solution of the laminar-turbulent transition. A mathematical model consists of the Reynolds-averaged Navier-Stokes equations, which are completed by the explicit algebraic Reynolds stress model (EARSM) of turbulence. The algebraic model of laminar-turbulent transition, which is integrated to the EARSM, is based on the work of Kubacki and Dick (Int. J. Heat Fluid Flow **58**, 68–83, 2016) where the turbulent kinetic energy is split in to the small-scale and large-scale parts. The algebraic model is simple and does not require geometry data such as wall-normal distance and all formulas are calculated using local variables. A numerical solution is obtained by the finite volume method based on the HLLC scheme and explicit Runge-Kutta method.

Keywords Laminar-turbulent transition · Algebraic model of transition · EARSM · Finite volume method

Mathematics Subject Classification (2010) 65M08 · 76N99 · 68U20

1 Introduction

The laminar-turbulent transition is important, yet still not fully resolved problem of the fluid dynamics. There are many models of transition available now ranging from simple algebraic models to complex two-equation models. Nevertheless, even the

Communicated by: Pavel Solin

✉ Jiří Holman
Jiri.Holman@fs.cvut.cz

Jiří Fürst
Jiri.Furst@fs.cvut.cz

[1] Department of Technical Mathematics, Faculty of Mechanical Engineering, Czech Technical University in Prague, Karlovo náměstí 13, Prague 2, 121 35, Czech Republic

most complicated two-equation transition models cannot be used for the solution of general transitional flows. This is caused by the complicated nature of the laminar-turbulent transition mechanism. The natural transition from laminar to turbulent state is caused by the instability of the Tollmien-Schlichting waves [2]. With a turbulence level above $0.5-1\%$, the free-stream turbulence induces the so-called Klebanoff distortions in the near-wall region of the boundary layer [1]. The Klebanoff distortions grow downstream and then break down, which leads to the formation of turbulent spots. This type of transition mechanism is called the bypass transition, because the instability mechanism of the Tollmien-Schlichting waves is bypassed. Another possible mechanism is the laminar boundary layer separation with low free-stream turbulence, where the transition is initiated by the inviscid Kelvin-Helmholtz instability. Since it is very difficult to formulate a transition model which would be able to reproduce all transition mechanisms correctly, it is reasonable to focus on some of them only.

The aim of this work is the modification of an algebraic model of bypass transition [1], which was originally combined with the Wilcox two-equation $k-\omega$ model. The algebraic model will be integrated to the EARSM of turbulence, which has generally better predictive capabilities than standard two-equation models of turbulence. The main difference between the EARSM and two-equation eddy-viscosity models is nonlinear relation between the tensor of Reynolds stresses and the strain-rate tensor and consequently nonlinear production terms in transport equations for turbulent quantities. Improved results, which have been obtained with aid of advanced modeling of turbulence by the EARSM, were published in several papers, e.g. [3–5] or [6] and also by other authors, e.g. [7] or [8].

2 Governing equations

Turbulent flow of compressible fluid is modeled by the set of averaged Navier-Stokes equations[1]

$$\frac{\partial \overline{\rho}}{\partial t}+\frac{\partial(\overline{\rho}\widetilde{u_j})}{\partial x_j}=0, \tag{1}$$

$$\frac{\partial(\overline{\rho}\widetilde{u_i})}{\partial t}+\frac{\partial(\overline{\rho}\widetilde{u_i}\widetilde{u_j})}{\partial x_j}+\frac{\partial \overline{p}}{\partial x_i}=\frac{\partial}{\partial x_j}\left(\overline{\tau_{ij}}+\tau_{ij}^t\right), \tag{2}$$

$$\frac{\partial(\overline{\rho}\widetilde{E})}{\partial t}+\frac{\partial}{\partial x_j}\left[(\overline{\rho}\widetilde{E}+\overline{p})\widetilde{u_j}\right]=\frac{\partial}{\partial x_j}\left[\left(\overline{\tau_{ij}}+\tau_{ij}^t\right)\widetilde{u_i}\right]-\frac{\partial}{\partial x_j}\left(\overline{q_j}+q_j^t\right). \tag{3}$$

The unknown variables are mean values of density $\overline{\rho}$, components of velocity vector $\widetilde{u_i}$, total specific energy $\widetilde{E}$[2], and static pressure $\overline{p}$, where the bar is indicating time average (Reynolds average) defined as

$$\overline{\Phi}(\vec{x},t)=\lim_{T\to\infty}\frac{1}{T}\int_t^{t+T}\Phi(\vec{x},\tau)d\tau \tag{4}$$

[1] Summation over repeated indices will be used throughout the paper.

[2] $\widetilde{E}=\widetilde{u}_e+\widetilde{u_j}\widetilde{u_j}/2+k$, where u_e is internal energy.

and the tilde indicates density-weighted average (Favre average) defined as

$$\widetilde{\Phi} = \frac{\overline{\rho \Phi}}{\overline{\rho}}. \tag{5}$$

The $\overline{\tau_{ij}}$ is the mean stress tensor. Assuming the Newtonian fluids only, the stress tensor components can be expressed as

$$\overline{\tau_{ij}} = \overline{\mu}\left(\frac{\partial \widetilde{u_i}}{\partial x_j} + \frac{\partial \widetilde{u_j}}{\partial x_i} - \frac{2}{3}\delta_{ij}\frac{\partial \widetilde{u_k}}{\partial x_k}\right), \qquad \overline{\mu} = \mu_{\text{ref}}\left(\frac{\rho_{\text{ref}}}{p_{\text{ref}}}\frac{\overline{p}}{\overline{\rho}}\right)^{\frac{3}{4}}, \tag{6}$$

where $\overline{\mu}$ is the mean viscosity computed using the Rayleigh relation with constants μ_{ref}, ρ_{ref}, and p_{ref}. The $\overline{q_j}$ and q_j^t are components of the mean heat flux vector and the turbulent heat flux vector respectively. The mean heat flux is obtained using Fourier's law while the turbulent heat flux is modeled as an analogy with heat flux as

$$\overline{q_j} = -\frac{\kappa}{\kappa - 1}\frac{\overline{\mu}}{Pr}\frac{\partial}{\partial x_j}\left(\frac{\overline{p}}{\overline{\rho}}\right), \qquad q_j^t = -\frac{\kappa}{\kappa - 1}\frac{\mu_t}{Pr_t}\frac{\partial}{\partial x_j}\left(\frac{\overline{p}}{\overline{\rho}}\right), \tag{7}$$

where Pr is the Prandtl number and Pr_t is the turbulent Prandtl number. Both dimensionless numbers are assumed constant[3] as well as κ, which is the specific heat ratio[4].

The μ_t and τ_{ij}^t are the turbulent viscosity and the Reynolds stress tensor respectively. Both terms have to be modeled by suitable model of turbulence.

Finally, the mathematical model is completed by the state equation of perfect gas that is formed

$$\overline{p} = (\kappa - 1)\left[\overline{\rho}\widetilde{E} - \frac{1}{2}\overline{\rho}\widetilde{u_j}\widetilde{u_j} - \overline{\rho}k\right], \tag{8}$$

where k is the turbulent kinetic energy which is also an unknown variable.

3 EARSM of turbulence

The explicit algebraic Reynolds stress model (EARSM) of Wallin and Johansson [8] is derived as a simplified solution of the full differential Reynolds stress transport model where both advection and diffusion are neglected under assumption of the weak equilibrium. The components of Reynolds stress tensor are given as

$$\tau_{ij}^t = \mu_t\left(\frac{\partial \widetilde{u_i}}{\partial x_j} + \frac{\partial \widetilde{u_j}}{\partial x_i} - \frac{2}{3}\delta_{ij}\frac{\partial \widetilde{u_k}}{\partial x_k}\right) - \frac{2}{3}\delta_{ij}\overline{\rho}k - \overline{\rho}k a_{ij}^{(ex)}, \tag{9}$$

where turbulent viscosity is given by relation

$$\mu_t = -\frac{1}{2}(\beta_1 + II_\Omega \beta_6)\overline{\rho}k\tau \tag{10}$$

[3] $Pr = 0.72$, $Pr_t = 0.9$.

[4] We assume perfect gas (the air) as a fluid, where $\kappa = 1.4$.

and extra anisotropy as

$$\begin{aligned} a_{ij}^{(ex)} = \quad & \beta_3\left(\Omega_{ik}^*\Omega_{kj}^* - \frac{1}{3}II_\Omega\delta_{ij}\right) \\ & + \beta_4(S_{ik}^*\Omega_{kj}^* - \Omega_{ik}^*S_{kj}^*) \\ & + \beta_6\left(S_{ik}^*\Omega_{kl}^*\Omega_{lj}^* + \Omega_{ik}^*\Omega_{kl}^*S_{lj}^* - II_\Omega S_{ij}^* - \frac{2}{3}IV\delta_{ij}\right) \\ & + \beta_9(\Omega_{ik}^*S_{kl}^*\Omega_{lm}^*\Omega_{mj}^* - \Omega_{ik}^*\Omega_{kl}^*S_{lm}^*\Omega_{mj}^*). \end{aligned} \tag{11}$$

The turbulent viscosity μ_t and extra anisotropy $a_{ij}^{(ex)}$ are nonlinear terms, which depends on the dimensionless strain-rate tensor and vorticity tensor,

$$S_{ij}^* = \frac{\tau}{2}\left(\frac{\partial\widetilde{u_i}}{\partial x_j} + \frac{\partial\widetilde{u_j}}{\partial x_i} - \frac{2}{3}\delta_{ij}\frac{\partial\widetilde{u_k}}{\partial x_k}\right), \quad \Omega_{ij}^* = \frac{\tau}{2}\left(\frac{\partial\widetilde{u_i}}{\partial x_j} - \frac{\partial\widetilde{u_j}}{\partial x_i}\right) \tag{12}$$

and on the related invariants $II_S = S_{kl}^*S_{lk}^*$, $II_\Omega = \Omega_{kl}^*\Omega_{lk}^*$ and $IV = S_{kl}^*\Omega_{lm}^*\Omega_{mk}^*$. Beta coefficients $\beta_1,\ldots,\beta_9$ are also nonlinear terms dependent on the invariants II_S, II_Ω, IV and also on the invariant $V = S_{kl}^*S_{lm}^*\Omega_{mn}^*\Omega_{nk}^*$ [8]. The time scale τ is defined as

$$\tau = \max\left(\frac{1}{\beta^*\omega},\ 6\sqrt{\frac{\overline{\mu}}{\beta^*\overline{\rho}k\omega}}\right), \tag{13}$$

where $\beta^* = 0.09$ is the turbulent model constant and specific dissipation rate ω is an unknown variable.

A described version of the EARSM is based on the transport equations of the two-equation k-ω TNT model [9]. The TNT model consists of transport equation for the turbulent kinetic energy

$$\frac{\partial(\overline{\rho}k)}{\partial t} + \frac{\partial(\overline{\rho}k\widetilde{u_j})}{\partial x_j} = \tau_{ij}^t\frac{\partial\widetilde{u_i}}{\partial x_j} - \beta^*\overline{\rho}k\omega + \frac{\partial}{\partial x_j}\left[\left(\overline{\mu} + \sigma^*\mu_t\right)\frac{\partial k}{\partial x_j}\right] \tag{14}$$

and transport equation for the specific dissipation rate

$$\frac{\partial(\overline{\rho}\omega)}{\partial t} + \frac{\partial(\overline{\rho}\omega\widetilde{u_j})}{\partial x_j} = \alpha\frac{\omega}{k}\tau_{ij}^t\frac{\partial\widetilde{u_i}}{\partial x_j} - \beta\overline{\rho}\omega^2 + \frac{\partial}{\partial x_j}\left[\left(\overline{\mu} + \sigma\mu_t\right)\frac{\partial\omega}{\partial x_j}\right] + C_d, \tag{15}$$

where C_d is a cross-diffusion term defined as

$$C_d = \sigma_d\frac{\overline{\rho}}{\omega}\max\left(\frac{\partial k}{\partial x_j}\frac{\partial\omega}{\partial x_j},\ 0\right) \tag{16}$$

and $\sigma^* = 1.01$, $\alpha = 0.553$, $\beta = 0.075$, $\sigma = 0.5$, and $\sigma_d = 0.52$ are turbulent model constants, which have been derived especially for conjunction with the EARSM relations [5].

4 Algebraic model of bypass transition

The algebraic model of laminar-turbulent bypass transition of Kubacki and Dick was originally integrated to the Wilcox $k-\omega$ model of turbulence [1]. The transition

model is based on the splitting of turbulent kinetic energy k to a small-scale part k_s and a large-scale part k_l by introducing shear sheltering factor f_{SS},

$$f_{SS} = \exp\left[-\left(\frac{C_{SS}\overline{\mu}\Omega}{\overline{\rho}k} \right)^2 \right], \tag{17}$$

$$k_s = f_{SS}k, \qquad k_l = k - k_s, \tag{18}$$

where $\Omega = \sqrt{2\Omega_{ij}\Omega_{ij}}$ is the vorticity tensor magnitude and C_{SS} is a constant. This concept is borrowed from the three-equation $k_T - k_L - \omega$ model of turbulence [10]. The small-scale disturbances, which contribute to the turbulence production by shear, are damped out in the vicinity of the laminar part of the boundary layer, while the large-scale disturbances are penetrating into the laminar layer which leads to induction of the Klebanoff distortions.

The turbulence production by shear is modeled with aid of the turbulent viscosity associated with the small-scale part of turbulent kinetic energy

$$\mu_s = -\frac{1}{2}(\beta_1 + II_\Omega \beta_6)\overline{\rho}k_s\tau. \tag{19}$$

The turbulent viscosity in the production terms of turbulence models (14) and (15) is replaced by the small-scale turbulent viscosity μ_s, i.e.,

$$P_k = \tau_{ij}^t \frac{\partial \widetilde{u}_i}{\partial x_j} \rightarrow \hat{P}_k = \hat{\tau}_{ij}^t \frac{\partial \widetilde{u}_i}{\partial x_j}, \tag{20}$$

$$P_\omega = \alpha \frac{\omega}{k} \tau_{ij}^t \frac{\partial \widetilde{u}_i}{\partial x_j} \rightarrow \hat{P}_\omega = \alpha \frac{\omega}{k} \hat{\tau}_{ij}^t \frac{\partial \widetilde{u}_i}{\partial x_j}, \tag{21}$$

where modified tensor of Reynolds stresses now reads

$$\hat{\tau}_{ij}^t = \mu_s \left(\frac{\partial \widetilde{u}_i}{\partial x_j} + \frac{\partial \widetilde{u}_j}{\partial x_i} - \frac{2}{3}\delta_{ij}\frac{\partial \widetilde{u}_k}{\partial x_k} \right) - \frac{2}{3}\delta_{ij}\overline{\rho}k_s - \overline{\rho}k_s a_{ij}^{(ex)}. \tag{22}$$

A second change to the EARSM is the multiplication of modified production term (20) in k-equation by intermittency factor γ, which is defined as

$$\gamma = \min(\ \max(Re_{k\Omega} - C_T,\ 0),\ 1\ ), \tag{23}$$

where C_T is a constant and the Reynolds number $Re_{k\Omega}$ which is given by relation

$$Re_{k\Omega} = \frac{\overline{\rho}k}{\overline{\mu}\Omega} \tag{24}$$

is the transition onset parameter [1].

Finally, to sum up all changes done to the EARSM, we begin with definition of the transition onset parameter $Re_{k\Omega}$ (24) and compute shear sheltering factor (17) and intermittency factor (23) with model constants $C_{SS} = 2.75$ and $C_T = 1.8125$. Then, the production terms in equations (14) and (15) are modified as

$$\hat{P}_k = \gamma f_{SS} P_k, \qquad \hat{P}_\omega = f_{SS} P_\omega. \tag{25}$$

The model constants C_{SS} and C_T have been adjusted from original values due to the described modifications (integration of the algebraic model of transition to different

models of turbulence and usage of transition onset parameter (24) which is independent of geometry). Both constants have been optimized for the correct transition onset in the most basic ERCOFTAC test case T3A (see Section 6).

5 Numerical method

The set of averaged Navier-Stokes equations together with the transport equations of the EARSM can be rewritten to the vector form

$$\frac{\partial W}{\partial t} + \frac{\partial F_j(W)}{\partial x_j} = \frac{\partial R_j(W)}{\partial x_j} + Q(W), \tag{26}$$

where $W = (\overline{\rho}, \overline{\rho}\widetilde{\vec{u}}, \overline{\rho}\widetilde{E}, \overline{\rho}k, \overline{\rho}\omega)^T$ is the vector of averaged conservative variables, F_j are inviscid fluxes, R_j are viscous fluxes, and vector Q contains source terms. The numerical solution is obtained by the in-house software based on a cell-centered finite volume method [11], which can be written in a semi-discrete form

$$\frac{dW_i}{dt} = \frac{1}{|D_i|} \sum_{k=1}^{\text{faces}} (\widehat{R}_k - \widehat{F}_k)\Delta S_k + Q(W_i), \tag{27}$$

where W_i is an averaged solution over the cell D_i, viscous flux $\widehat{R} = \vec{R} \cdot \vec{n}$, inviscid flux $\widehat{F} = \vec{F} \cdot \vec{n}$, ΔS is area of the cell face between two adjacent cells, and $\vec{n}$ is unit vector normal to face.

The inviscid flux is approximated by the HLLC Riemann solver [12] with the piece-wise linear MUSCL reconstruction of the primitive variables. The viscous flux is discretized by the central scheme with aid of diamond-shaped dual cells. Time integration of the semi-discrete finite volume method (27) is done by the explicit two-stage TVD Runge-Kutta method with point implicit treatment of the source terms [3].

6 Numerical solution of ERCOFTAC T3 cases

The presented model has been tested on the ERCOFTAC T3 flat plate flow cases [13]. Three different cases have been considered. The T3A case has moderate inlet turbulence intensity, the T3A- has low let turbulence intensity, while the T3B case is characterized by high inlet turbulence level (see Table 1). All cases have zero streamwise pressure gradient.

Table 1 Summary of inlet conditions for the T3 cases

ERCOFTAC ZPG flat plate flow cases					
Case	U[m/s]	Tu [%]	μ_t/μ	μ[kg/ms]	ρ [kg/m^3]
T3A	5.4	3.3	12	$1.8{\cdot}10^{-5}$	1.2
T3B	9.4	6.5	100	$1.8{\cdot}10^{-5}$	1.2
T3A-	19.8	0.874	8.72	$1.8{\cdot}10^{-5}$	1.2

Table 2 Prescribed inlet boundary conditions for the T3 cases

Inlet boundary conditions at $x = -0.05$m			
Case	$k_\infty [m^2 s^{-2}]$	Tu [%]	ω_∞ $[s^{-1}]$
T3A	0.061	3.73	324.2
T3B	0.680	7.16	438.7
T3A-	0.049	0.91	367.3

All cases were solved on a rectangular domain ($-0.05 \leq x[m] \leq 2.9, 0 \leq y[m] \leq 0.175$) which was covered by structured mesh with 635×105 cells. Leading edge of the flat plate is placed at point [0, 0]. The mesh was refined in the vicinity of the leading edge and also in the wall-normal direction, where $y_1^+ < 1$ holds. Boundary conditions were set in the following way:

- Inlet [$x = -0.05$, $y \in (0, 0.175)$], prescribed density, components of velocity vector, turbulent energy, and specific dissipation rate.
- Outlet [$x = 2.9$, $y \in (0, 0.175)$], prescribed static pressure.
- Adiabatic wall (flat plate) [$x \in (0, 2.9)$, $y = 0$].
- Symmetry [$x \in (-0.05, 0)$, $y = 0$] and [$x \in (-0.05, 2.9)$, $y = 0.175$].

Table 2 shows values of inlet turbulent quantities which were calculated using analytical solution of simplified turbulence model for the case of decaying turbulent kinetic energy

$$\frac{dk}{dt} = -\beta^* k\omega, \qquad \frac{d\omega}{dt} = -\beta\omega^2. \tag{28}$$

Initial conditions were chosen according to the leading edge values (see Table 1).

Numerical solutions were obtained using in-house FVM code described in Section 5.

Figure 1 shows the friction coefficient distribution for the T3A case. The presented model predicts transition onset very well, but transition is faster than in experiment. This behavior is also apparent in the case T3A- (Fig. 5). On the other hand, pure EARSM without the algebraic model of transition predicted transition onset very early with transition length longer than that in the experiment. Distribution of the local free-stream turbulence intensity is on Fig. 2. One can see very good match of both standard and modified EARSM with experiment.

Figures 3 and 4 show results for the T3B case. The presented model predicts transition onset in this case to early. Free-stream turbulence intensity level is very high in this case and even much more complicated transition models (such as two-equation $\gamma - Re_{\theta t}$ model [14]) are unable to predict correct transition onset. The pure EARSM predicts transition onset even earlier with transition length much longer than in experiment. Distributions of the local free-stream turbulence intensity (Fig. 3) are again predicted very well .

Figure 5 shows the friction coefficient distribution for the T3A- case. The transition onset shifted slightly downstream and the transition length seems to be slightly shorter. Pure EARSM again predicts transition onset to early with transition length much longer than in experiment. Distributions of the local free-stream turbulence intensity (Fig. 6) are in good agreement with experiment.

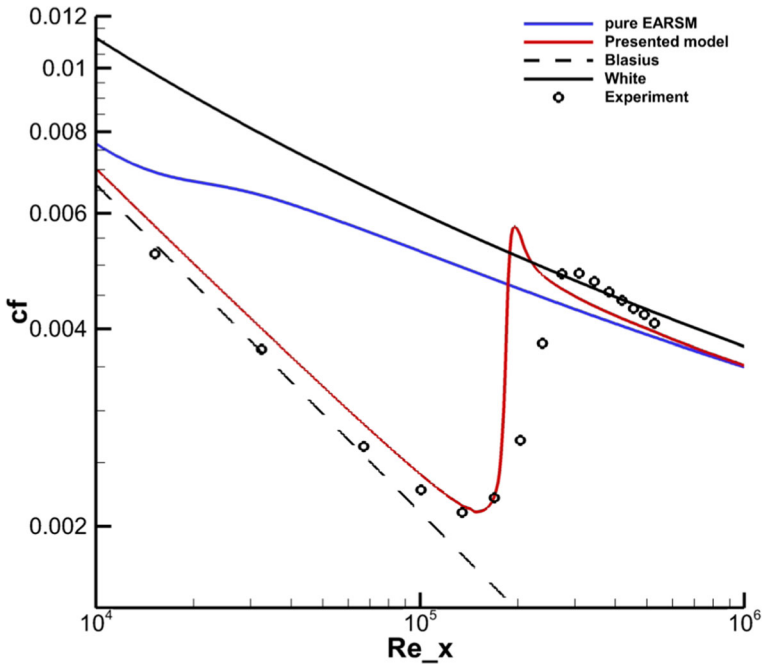

Fig. 1 Distribution of friction coefficient, case T3A

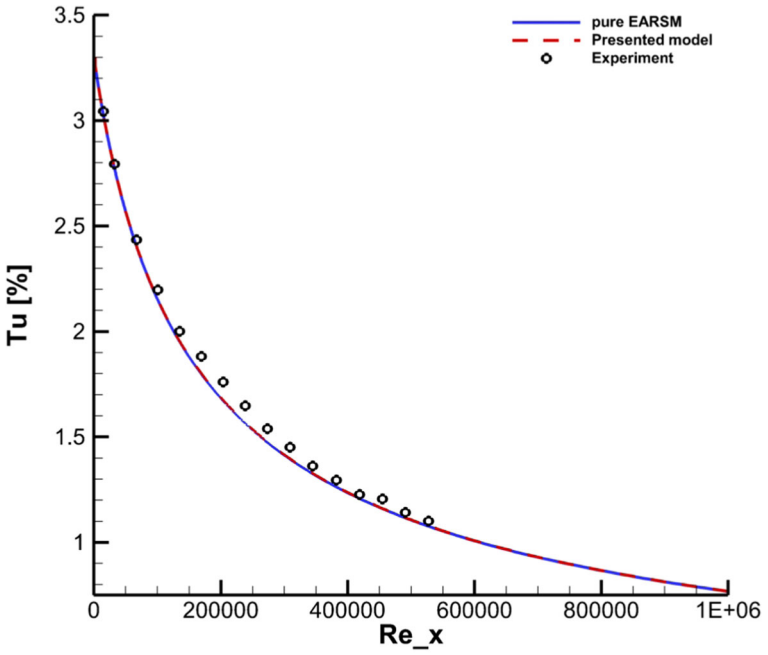

Fig. 2 Distribution of turbulence intensity, case T3A

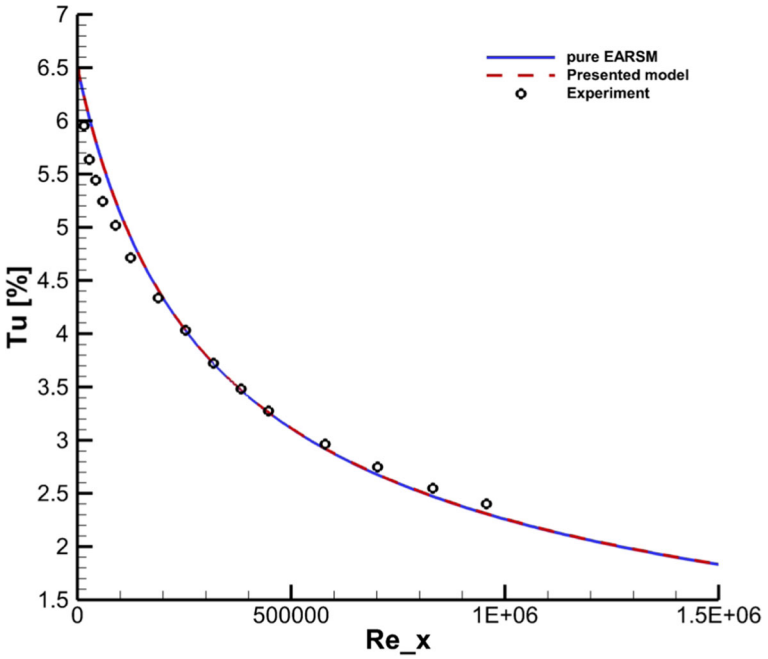

Fig. 3 Distribution of turbulence intensity, case T3B

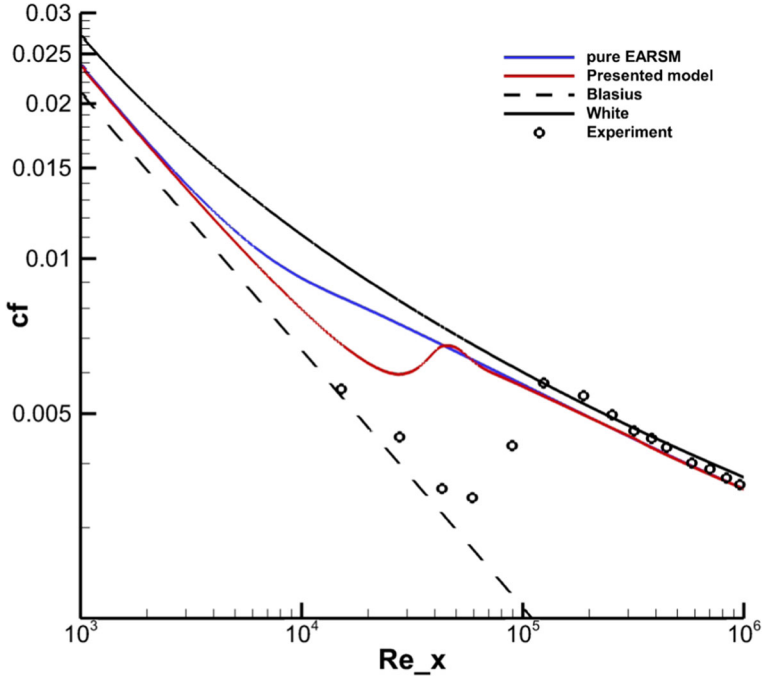

Fig. 4 Distribution of friction coefficient, case T3B

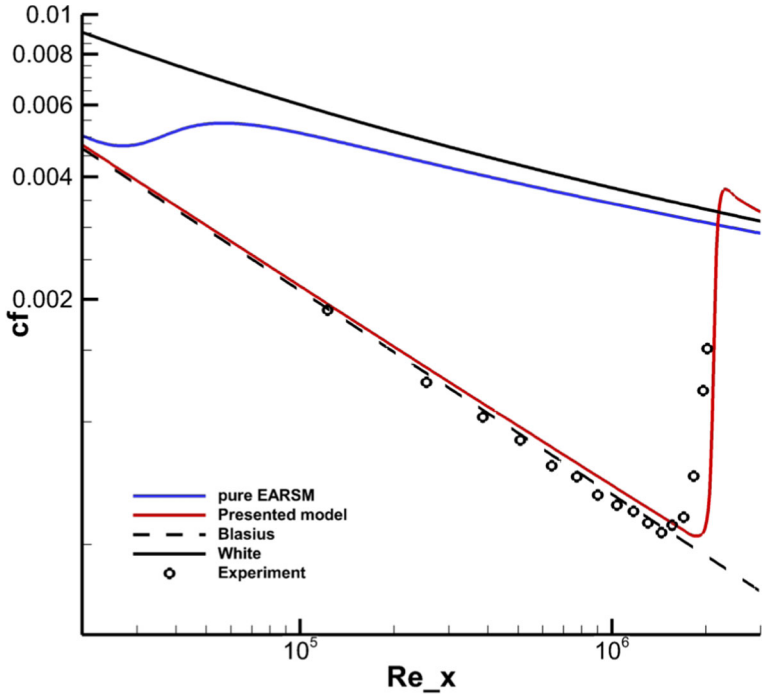

Fig. 5 Distribution of friction coefficient, case T3A-

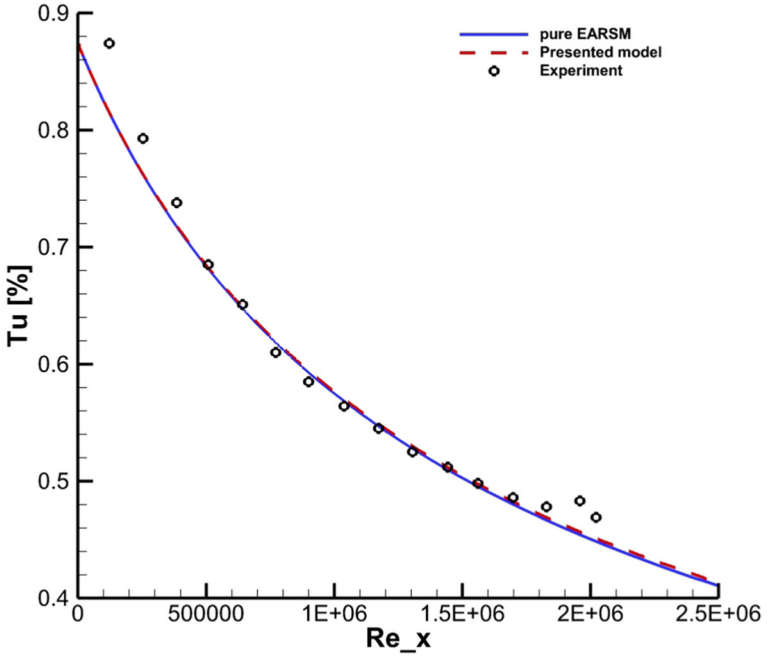

Fig. 6 Distribution of turbulence intensity, case T3A-

From the obtained results, one can conclude that the presented model is a significant improvement over the pure EARSM. It is able to predict correct transition onset for low to medium free-stream turbulence intensity. The transition process is predicted faster, but still with smaller error than in the case of the pure EARSM without an algebraic model of transition.

7 Subsonic flow past NACA0012 airfoil

This section deals with subsonic flow of air past the NACA0012 airfoil. This case is characterized by the free-stream Mach number $M_\infty = 0.225$, Reynolds number $Re = 5 \cdot 10^5$, inlet angle of attack $\alpha_\infty = 0°$, and free-stream turbulence intensity $Tu = 1\%$. The problem was solved on the domain approximately 30 times larger than airfoil chord $c = 0.1$m. The domain was covered by a structured hyperbolic mesh (Fig. 7) composed of 480×100 cells with 400 cells around the airfoil. A numerical solution was obtained using an in-house FVM code described in Section 5.

Figure 8 shows distribution of the Mach number in form of isolines. Figures 9 and 10 show a comparison of pressure and friction coefficient distributions obtained by the presented model and the XFOIL software, which is programmed for analysis of subsonic isolated profiles where transition is modeled by the e^N method [15]. One can see good match between two entirely different methods. The presented model

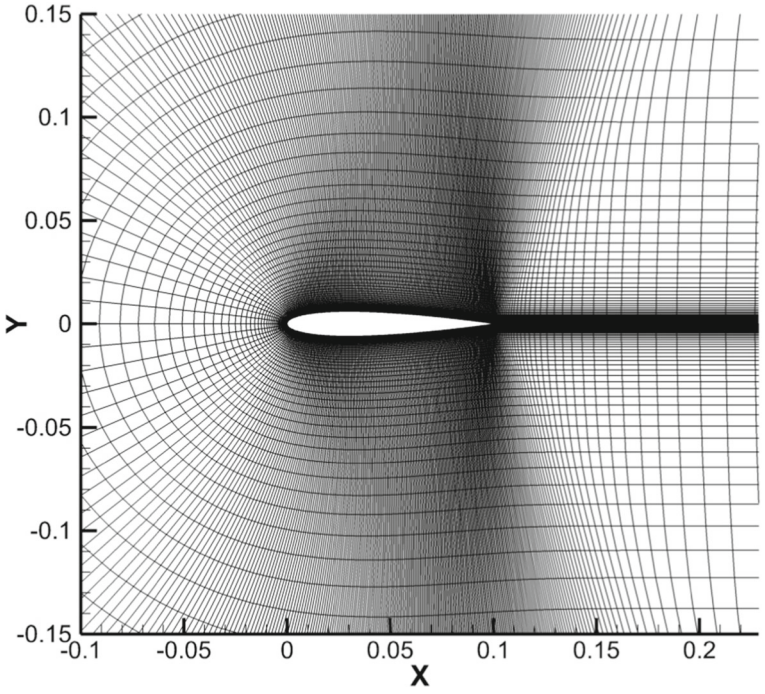

Fig. 7 Computational grid in the vicinity of the airfoil.

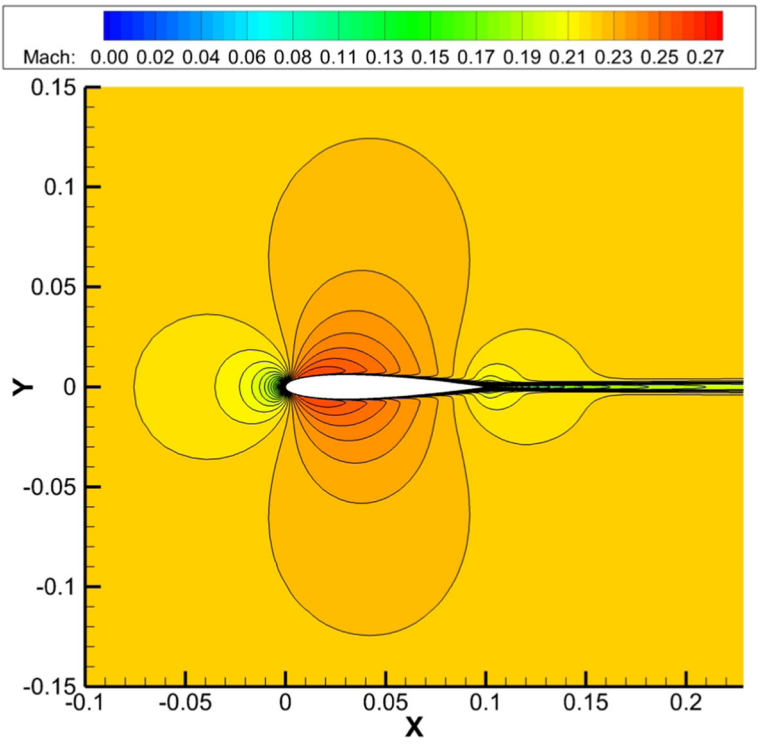

Fig. 8 Distribution of Mach number

predicted transition onset correctly, while the transition length is slightly shorter in comparison with the XFOIL. In contrast, pure unmodified EARSM predicted transition onset almost immediately. This had negative effect on friction coefficient values, which are predicted slightly lower than with presented model or XFOIL software.

Figures 9 and 10 also show comparison with the γ-SST transition model [18], which predicted transition onset much further downstream.

8 Transonic flow through the VKI nozzle blade cascade

The last section presents the numerical solution of transonic flow through the VKI nozzle blade cascade. The problem is characterized by the outlet isoentropic Mach number $M_{2is} = 1.089$, Reynolds number $Re = 2.11 \cdot 10^6$, inlet angle of attack $\alpha_\infty = 0°$, and free-stream turbulence intensity $Tu = 6.6\%$. This setting corresponds to the test MUR241 [16]. Since the blade cascade is periodic, the computational domain is chosen as a one period (Fig. 11). The computational mesh is unstructured with total number of 62,011 cells with refinement in the vicinity of the blade surface (see Fig. 11). The simulation was carried out in software package OpenFOAM with

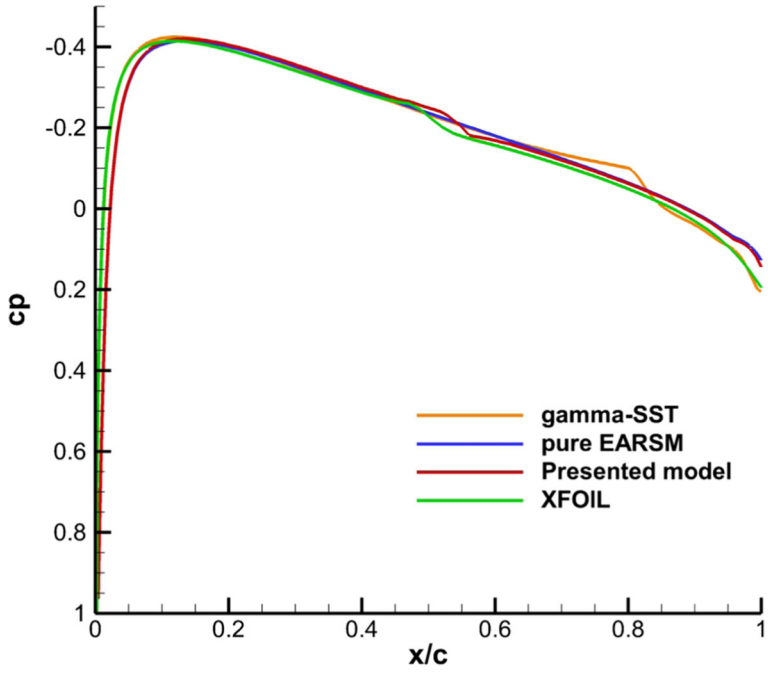

Fig. 9 Distribution of pressure coefficient

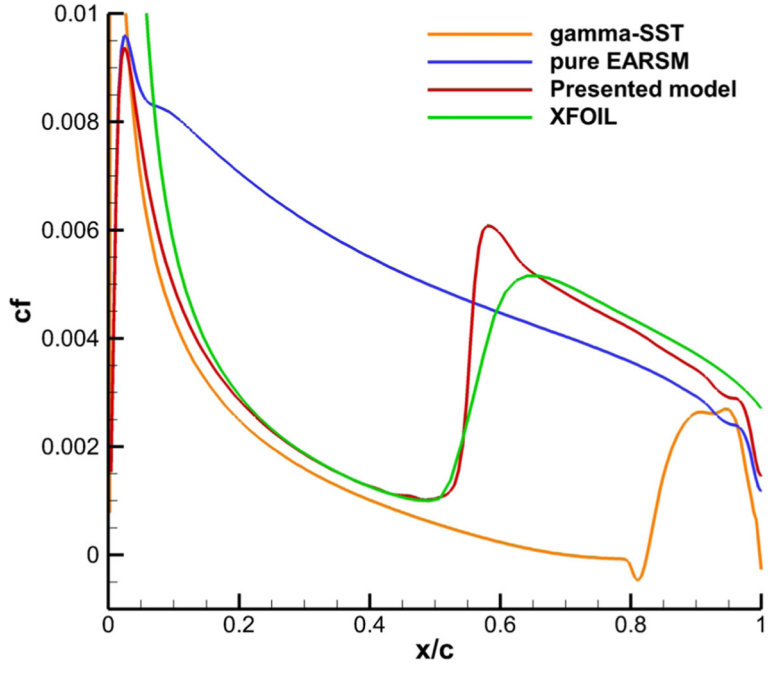

Fig. 10 Distribution of friction coefficient

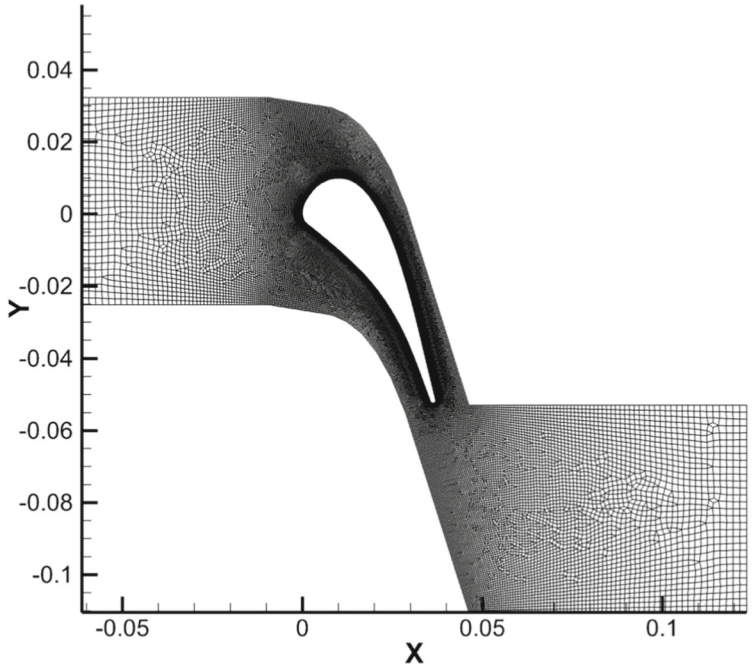

Fig. 11 Computational domain and grid

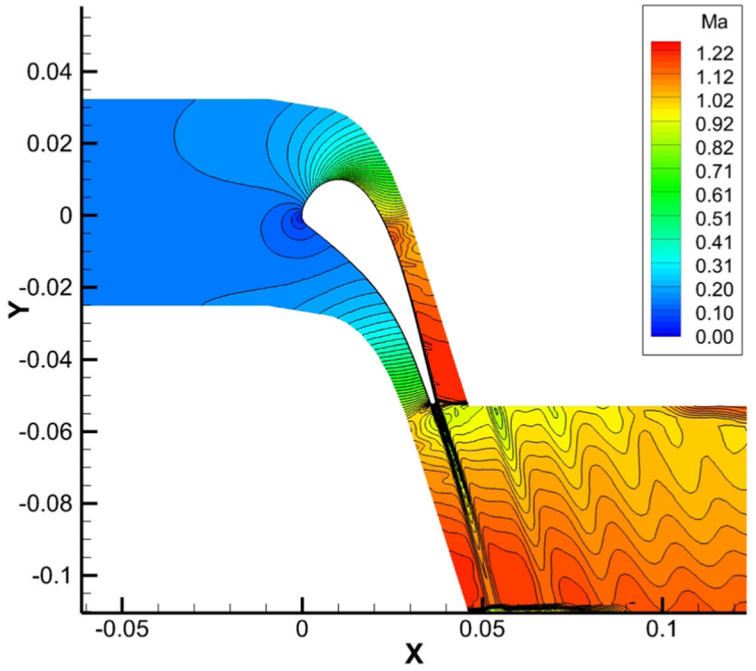

Fig. 12 Distribution of Mach number

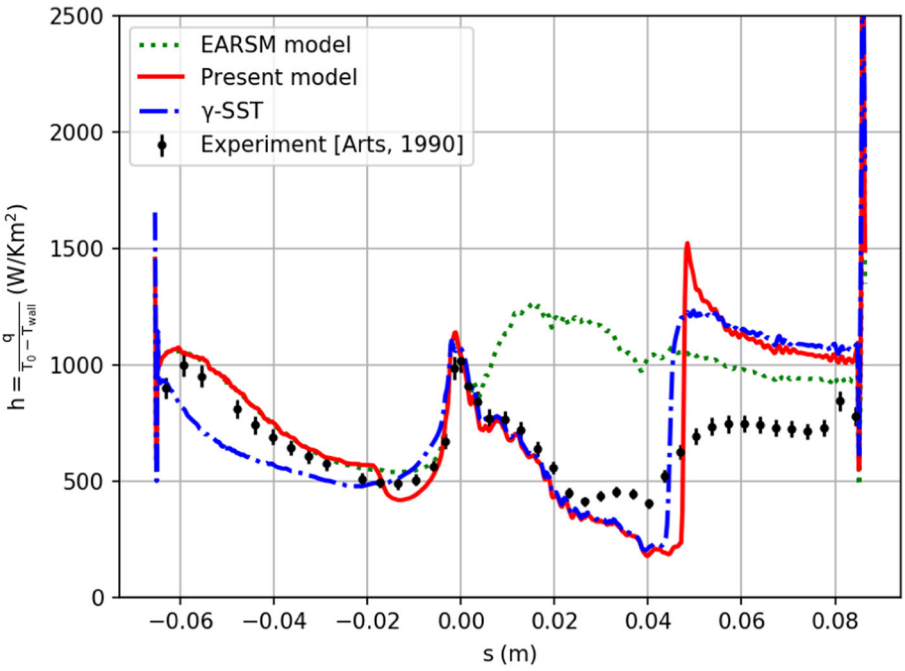

Fig. 13 Distribution of heat flux. Leading edge is located in point $s = 0$, pressure side of the blade is $s \in (s_{\min}, 0)$, suction side of the blade is $s \in (0, s_{\max})$

custom solver, which is based on the implicit lower-upper symmetric Gauss-Seidel method and AUSM+up scheme [17].

Figure 12 shows distribution of the Mach number in form of isolines. Figure 13 shows a comparison of heat flux distributions. The presented model predicted transition onset almost in the same spot as a one-equation γ transition model combined with the SST $k - \omega$ model of turbulence [18]. Both models are in good agreement with experiment, even though transition length is moderately shorter. Both models also overpredict heat transfer at the suction side in the turbulent part of boundary layer, where the presented model is slightly closer to experiment. Pure EARSM on the other hand predicted transition onset very early, but overprediciton of heat transfer is moderately smaller.

9 Conclusion

The algebraic model of laminar-turbulent bypass transition, which was originally combined with the Wilcox $k - \omega$ model of turbulence, has been successfully integrated to the EARSM. While the presented model cannot be considered as a general model for transitional flows, it can be used for the simulations of bypass transition in relative wide range of technical applications. The model is also relatively simple, local, independent of solved geometry, and easy to implement.

Funding information The authors acknowledge the financial support from the EU Operational Programme Research, Development and Education, and from the Center of Advanced Aerospace Technology (CZ.02.1.01/0.0/0.0/16_019/0000826), Faculty of Mechanical Engineering, Czech Technical University in Prague.

References

1. Kubacki, S., Dick, E.: An algebraic model for bypass transition in turbomachinery boundary layer flows. Int. J. Heat Fluid Flow **58**, 68–83 (2016)
2. Schlichting, B., Gersten, K.: Boundary Layer Theory, 8th Revised and Enlarged Edition. Springer, Berlin (2000)
3. Holman, J., Fürst, J.: Comparison of EARSM and TNT models for the case of transonic flows. Topical Problems of Fluid Mechanics 2008, 47–50 (2008)
4. Holman, J., Fürst, J.: Recalibration of TNT model for conjunction with EARSM model of turbulence, Topical Problems of Fluid Mechanics 2012, pp. 43–46
5. Holman, J., Fürst, J.: Numerical Simulation of Compressible Turbulent Flows Using Modified EARSM model, Numerical Mathematics and Advanced Applications - ENUMATH 2013, pp. 677–689. Springer (2014)
6. Holman, J.: Unsteady Flow past a Circular Cylinder Using Advanced Turbulence Models. Appl. Mech. Mater. **821**, 23–30 (2016)
7. Hellsten, A.: New two-equation turbulence model for aerodynamics applications, Report A-21 Helsinki University of Technology (2004)
8. Wallin, S.: Engineering turbulence modeling for CFD with focus on explicit algebraic Reynolds stress models, dissertation thesis, Royal Institute of Technology (2000)
9. Kok, J.C.: Resolving the Dependence on Freestream Values for $k-\omega$ Turbulence Model. AIAA J. **38**, 7 (2000)
10. Lopez, M., Walters, D.K.: A Recommended Correction to the $k_T-k_L-\omega$ Transition-Sensitive Eddy-Viscosity Model. J. Fluids Eng. [online] **139**(2), 024501 (2016). ISSN 0098-2202
11. Leveque, R.J.: Finite-Volume Methods for Hyperbolic Problems. Cambridge University Press, Cambridge (2004)
12. Batten, P., Leschziner, M.A., Goldberg, U.C.: Average-State Jacobians and implicit methods for compressible viscous and turbulent flows. J. Comput. Phys. **137**, 38–78 (1997)
13. Savill, A.M.: Predicting by-pass transition with turbulence models, 11th Australasian Fluid Mechanics Conference, pp. 14–18. University of Tasmania, Hobart (1992)
14. Langtry, R., Menter, F.R.: Overview of industrial transition modelling in CFX technical report. ANSYS (2006)
15. Drela, M.: XFOIL: An analysis and design system for low Reynolds number airfoils. In: Mueller, T.J. (ed.) Low Reynolds Number Aerodynamics [online], pp. 1–12. Lecture Notes in Engineering (1989)
16. Arts, T., Lambert de Rouvroit, M., Rutherford, A.W.: Aero-thermal investigation of a highly loaded transonic linear turbine guide vane cascade: a test case for inviscid and viscous flow computations, pp. 174. VKI technical note (1990)
17. Fürst, J.: Development of a coupled matrix-free LU-SGS solver for turbulent compressible flows. Comput. Fluids [online] **172**, 332-339 (2018). ISSN 00457930
18. Menter, F.R., Smirnov, P.E., Liu, T., Avancha, R.: A one-equation local correlation-based transition model. Flow Turbul. Combust. [online] **95**(4), 583–619 (2015). ISSN 1386-6184